Molecular Phylogenetics and Evolution 59 (2011) 89–102

Contents lists available at ScienceDirect

Molecular Phylogenetics and Evolution

journal homepage: www.elsevier.com/locate/ympev

Reconciling phylogeography and ecological niche models for New Zealand beetles: Looking beyond glacial refugia

Katharine A. Marske [a,b,*], Richard A.B. Leschen [a], Thomas R. Buckley [a]

[a] Landcare Research, Private Bag 92170, Auckland 1142, New Zealand
[b] Center for Macroecology, Evolution and Climate, University of Copenhagen, Universitetsparken 15, DK-2100 Copenhagen Ø, Denmark

ARTICLE INFO

Article history:
Received 19 July 2010
Revised 12 November 2010
Accepted 13 January 2011
Available online 22 January 2011

Keywords:
Colydiinae
Epistranus lawsoni
Pristoderus bakewelli
Maxent
Coalescent phylogeography
BEAST

ABSTRACT

Mitochondrial DNA (*cox1*) sequence data and recently developed coalescent phylogeography models were used to construct geo-spatial histories for the New Zealand fungus beetles *Epistranus lawsoni* and *Pristoderus bakewelli* (Zopheridae). These methods utilize continuous-time Markov chains and Bayesian stochastic search variable selection incorporated in BEAST to identify historical dispersal patterns via ancestral state reconstruction. Ecological niche models (ENMs) were incorporated to reconstruct the potential geographic distribution of each species during the Last Glacial Maximum (LGM). Coalescent analyses suggest a North Island origin for *E. lawsoni*, with gene flow predominately north–south between adjacent regions. ENMs for *E. lawsoni* indicated glacial refugia in coastal regions of both main islands, consistent with phylogenetic patterns but at odds with the coalescent dates, which implicate much older topographic events. Dispersal matrices revealed patterns of gene flow consistent with projected refugia, suggesting long-term South Island survival with population vicariance around the Southern Alps. Phylogeographic relationships are more ambiguous for *P. bakewelli*, although long-term survival on both main islands is evident. Divergence dates for both species are consistent with the topographic evolution of New Zealand over the last 10 Ma, whereas the signature of the LGM is less apparent in the time-scaled phylogeny.

1. Introduction

The practice of phylogeography has often been criticized for its application as a descriptive integration of phylogenies and environmental phenomena, without explicit ecological or geological data (Kidd and Ritchie, 2006; Carstens and Richards, 2007). One popular response has been the adoption of paleoclimate models, or ecological niche models (ENMs) projected onto historical landscapes (e.g., Hugall et al., 2002), which provide a spatial context for phylogeographic results or generate testable hypotheses (Carstens and Richards, 2007; Waltari et al., 2007). These combined studies have been widely utilized to identify refugia during the late-Pleistocene Last Glacial Maximum (LGM) (e.g., Hugall et al., 2002; Carstens and Richards, 2007; Buckley et al., 2009; Marske et al., 2009). Few studies present discrepancies between methods—due to time-frame mismatch or ambiguous or conflicting results—and rarely do such conflicts occur (Waltari et al., 2007). Here we illustrate the interpretive challenge posed by ambiguous relationships between phylogenies and ENMs while attempting to infer the biogeographic history of two taxa from a geologically and climatically dynamic environment.

New Zealand is a particularly interesting setting for phylogeography studies because of its turbulent geological history, especially over the last 10 million years (King, 2000). Movement along the Pacific and Australian plate boundaries during the Miocene initiated uplift of the South Island mountain ranges (King, 2000) and southward draining of the Manawatu Strait which had inundated the lower North Island since the Oligocene (Bunce et al., 2009). Fiordland and Nelson, formerly adjacent, have undergone approximately 500 km of displacement along the Alpine Fault over the last 29 Ma (Bunce et al., 2009). The Southern Alps formed <12 Ma, with uplift accelerating 5 Ma (King, 2000), followed by Plio-Pleistocene uplift of the lower North Island ranges (Pulford and Stern, 2004). Progressive glacial cooling began during the late Pliocene (3.0–2.5 Ma) and intensified through the Pleistocene (Naish, 2005). New Zealand's LGM, 34,000–18,000 cal. year BP (Alloway et al., 2007), featured piedmont and valley glaciers along the Southern Alps from Fiordland to north Westland (Vandergoes and Fitzsimons, 2003) and a 120 m drop in sea level (Lambeck et al., 2002; Naish, 2005) connecting the North and South Islands between Taranaki and Nelson (King, 2000), and is believed to have restricted New Zealand's temperate

* Corresponding author at: Center for Macroecology, Evolution and Climate, University of Copenhagen, Universitetsparken 15, DK-2100 Copenhagen Ø, Denmark. Fax: +45 35321250.
E-mail addresses: kamarske@bio.ku.dk (K.A. Marske), leschenr@landcareresearch.co.nz (R.A.B. Leschen), buckleyt@landcareresearch.co.nz (T.R. Buckley).

1055-7903/$ - see front matter © 2011 Elsevier Inc. All rights reserved.
doi:10.1016/j.ympev.2011.01.005

biota into northern refugia on both islands, although the full extent of forest distribution is unknown (Alloway et al., 2007).

This history, with its wealth of biogeographic hypotheses, makes it challenging to tease apart the influences of various geological and climate events on the continent's biota, as demonstrated in a recent review of New Zealand's phylogeographic literature (Wallis and Trewick, 2009). Previous phylogenetic studies of the forest litter fauna from New Zealand and elsewhere suggest that these organisms experience population structuring across a fine spatial scale (Garrick et al., 2004; Sunnucks et al., 2006; Boyer et al., 2007; Marske et al., 2009). We have applied a variety of phylogeographic methods, including coalescent ancestral state reconstruction (Lemey et al., 2009), to unravel the spatial history of two New Zealand forest beetles: *Epistranus lawsoni* (Sharp) and *Pristoderus bakewelli* (Pascoe) (Zopheridae: Colydiinae). Both species are flightless, mycophagous, inhabit dead wood ecosystems and are widely distributed within New Zealand. Specifically, we aim to (a) identify LGM refugia for both species, (b) determine whether recent glaciation or older geological events were more important in shaping the distribution of genetic diversity in these species, and (c) address the resolution between ENMs and phylogeographic results with ambiguous temporal overlap.

2. Methods

2.1. Taxon sampling

The New Zealand Zopheridae are currently in a state of taxonomic flux due to the number of synonymies requiring formalization, and doubts about the present taxonomic limits of the genera (N. Lord, R. Leschen & T. Buckley, unpublished). Examination of type material and dissections show that the seven named species of New Zealand *Epistranus* should be considered as a single taxon, and five New Zealand *Pristoderus* species are synonyms of *P. bakewelli* (R. Leschen, unpublished). The New Zealand *Epistranus* are morphologically similar, and all are part of the leaf litter fauna, feeding on resupinate polyporoid and corticioid fungi growing on small diameter dead wood. Morphological variation is larger in the *P. bakewelli* group, where all forms occur on dead logs, and the range of variation may be associated with differential development in these woody habitats as seen in other dead wood feeders (reviewed in Walczyńska et al. (2010)).

E. lawsoni and *P. bakewelli* were collected throughout the North and South Islands by direct inspection of dead logs and woody debris, and by crumbling and sifting leaf and wood litter for Berlese or Winkler funnel extraction. *P. bakewelli* was also collected by beating thin woody stems and inspecting large logs at night. Specimens were also obtained from the ethanol collection at the Field Museum of Natural History, Chicago, including *P. bakewelli* from the Chatham Islands, an archipelago approximately 800 km east of mainland New Zealand. Locality data for ENMs were taken from these specimens and from pinned holdings with detailed label data (e.g., specific localities which could be pinpointed on a topographic map) in the New Zealand Arthropod Collection, Field Museum and the private collection of J. Nunn.

2.2. DNA extraction, amplification and sequencing

Genomic DNA was extracted using either the PureLink™ Genomic DNA MiniKit (Invitrogen, Carlsbad, CA, USA) or the X-tractor Gene™ CAS-1820 (Corbett Robotics, Brisbane, Australia) following digest. *E. lawsoni* were carefully broken in half behind the pronotum and the entire specimen was placed in extraction buffer and retained post-digest. Three legs were removed from each *P. bakewelli* and ground for digest. The 3′ end of the mitochondrial cytochrome oxidase subunit I (*cox1*) gene region was amplified using the primers C1-J-2183 (*E. lawsoni*) or C1-J-2195 (*P. bakewelli*) and TL2-N-3014 (Simon et al., 1994) according to the protocol in Marske et al. (2009). PCR products were purified using the MinElute 96 UF Plate (Qiagen, Venlo, Netherlands), eluting in 50 μL water. Sequence data collection, alignment and editing were as in Marske et al. (2009).

2.3. Population statistics

Summary statistics (Table 1) were calculated using DnaSp 4.5 (Rozas et al., 2003). The number of substitutions between sequences and the average number of substitutions between and within populations (localities from which two or more specimens were sequenced) were calculated in MEGA 4 (Tamura et al., 2007). The best-fit model of sequence evolution for each full data set was determined using the Akaike Information Criterion (AIC) implemented in Modeltest 3.7 (Posada and Crandall, 1998) with likelihood values calculated in PAUP* 4.0b10 (Swofford, 1998), and corrected pairwise genetic distance was calculated in PAUP* under the resulting model (GTR + I + Γ for both taxa). A Mantel test was conducted to test for matrix correlation between geographical and genetic distance (Fst), using the Isolation by Distance Web Service 3.16 (Jensen et al., 2005). Geographic distances between groups were calculated using Hawth's Tools 3.79 (Beyer, 2004) for ArcGIS 9.2 (Environmental Systems Research Institute, Redlands, CA, USA). For *P. bakewelli*, Chatham Islands sequences were treated as a single locality, and the test was performed with them included and excluded.

Analysis of molecular variance (AMOVA; Excoffier et al., 1992) was used to test the amount and significance of variance among regions delimited by various biogeographic hypotheses, compared to that among and within populations in individual biogeographic regions. We compared molecular variance on the North vs. South Islands, among five biotic zones (Wardle, 1963; 2 North, 3 South), and west vs. east of the Southern Alps on the South Island (e.g., Hill et al., 2009), for both species (Fig. 1a). For *E. lawsoni*, we also tested for differences between the two North Island biotic zones, among the three South Island biotic zones, and inside vs. outside of hypothesized LGM glacial refugia (Alloway et al., 2007), with "refugia" including localities along the Karamea coast (South Island) and north of the base of the Coromandel Peninsula (North Island) (Fig. 1). For *P. bakewelli*, we compared the lower North Island vs. the upper South Island biotic zones, as these areas were the best sampled. All AMOVAS were performed using Arlequin 3.1 (Excoffier et al., 2005), using 10,000 permutations. Individual collecting localities were treated as populations, and each population consisted of 1–4 haplotypes. The number of populations compared in each test is listed in Table 2, broken down by region.

2.4. Phylogenetic and molecular clock analysis

The best-fit model of sequence evolution was determined for individual codon positions (1 + 2 and 3). This yielded HKY + I + Γ (1 + 2) and GTR + I + Γ (3) for *E. lawsoni* and TIM + I + Γ (1 + 2) and GTR + I + Γ (3) for *P. bakewelli*. However, GTR + I + Γ had the next highest likelihood and AIC scores for *P. bakewelli* positions 1 + 2, and as these were extremely similar to those for TIM + I + Γ, we chose to use GTR + I + Γ in all analyses for easier implementation.

Molecular clock analyses were conducted in BEAST 1.5.3 (Drummond and Rambaut, 2007) under a Bayesian coalescent framework. As no external calibration points exist, we used two different rates of invertebrate mitochondrial DNA evolution: the widely used Brower (1994) rate of 2.3% My^{-1}, and Papadopoulou et al.'s (2010) rate of 3.54% My^{-1}, calibrated for flightless tenebrionid beetles. MCMC simulations were performed using a strict molecular clock,

Table 1
Sequence and population statistics for *E. lawsoni* and *P. bakewelli*.

	Epistranus lawsoni	*Pristoderus bakewelli*
No. individuals	168	88
No. localities	78	53
Polymorphic sites	350	248
Parsimony-informative sites	322	227
No. haplotypes	116	77
Haplotype diversity	0.9942 (sd = 0.001)	0.997 (sd = 0.002)
Nucleotide diversity (per site)	0.16194 (sd = 0.00258)	0.09858 (sd = 0.00157)
Tajima's *D*	0.36113, $P > 0.10$	−0.02922, $P > 0.10$
Fu and Li's *D*	1.06646, $P > 0.10$	0.75227, $P > 0.10$
Fu and Li's *F*	0.86314, $P > 0.10$	0.75227, $P > 0.10$
Mean pairwise genetic distance (corrected)	0.7651	0.2381
Max pairwise genetic distance (corrected)	1.8642	0.5712

under both the constant size and exponential growth population models. BEAST profiles incorporated a random starting tree and a normal prior on clock rate, using either the faster (mean = 0.0177, sd = 0.00177) or slower (mean = 0.0115, sd = 0.00115) substitution rate. All analyses incorporated the following priors: root height (exponential, mean = 1.0), GTR substitution rate matrix (Jeffrey's), alpha parameter for among-site rate variation (exponential, mean = 1), proportion of invariable sites (uniform, 0–1), and population size (exponential, mean = 1.0). For *E. lawsoni*, the HKY model priors for μ and κ had exponential (mean = 1.0) distributions. Under the exponential growth model, coalescent growth rate (uniform) was used. Analyses using the slower rate of 2.3% My^{-1} were repeated under a relaxed clock, for constant size and exponential growth models, with priors as above (clock rate normal, mean = 0.0115, sd = 0.00115), and exponential priors on coefficient of variation and covariance (mean = 1.0).

Each profile ran five times for 20 million generations, logging every 1000 generations. To choose between the constant size and exponential growth models for each species, log files were imported into Tracer 1.4 (Rambaut and Drummond, 2007) to determine whether the marginal posterior distribution of the growth rate parameter included zero. Tree files were combined using LogCombiner (Drummond and Rambaut, 2007) (burnin = 2000; thinning interval = 2000) and TreeAnnotator (Drummond and Rambaut, 2007) to yield a consensus tree for each set of analyses.

2.5. Phylogeographic reconstruction

Phylogeographic relationships between tree tip localities were estimated using the continuous-time Markov chains (CTMCs) and Bayesian stochastic search variable selection (BSSVS) applications in BEAST 1.5.2 (Lemey et al., 2009). As a coalescent implementation of ancestral state reconstruction, geographic regions were inferred as "states", which were mapped across the time-scaled phylogeny to infer the location of ancestral nodes. Rates of state-transition, or migration or dispersal between locations, were identified using Bayes factors, and a Bayes factor test was used to identify regions connected by significant state-transition throughout the phylogeny (Lemey et al., 2009).

Ancestral state reconstructions were executed under the constant size population models using the 3.54% My^{-1} rate for both species. Geographic regions inferred as "states" are highlighted in Fig. 1a, although for *P. bakewelli*, the single Taranaki sequence was included in Manawatu. Prior distributions were as above, with the addition of exponential geographic priors after Lemey et al. (2009). Tree files from five runs were combined (burnin = 2000; thinning interval = 5000) to generate a consensus tree for each species. Discrete rate matrices of geographic state transition were combined (burnin = 2000) from all five runs, and a Bayes factor test (script available at BEAST website) was applied, with Bayes factor >3 indicating well-supported diffusion rates between states.

2.6. Ecological niche modeling

Climate data used to construct the ENM included mean annual rainfall (mm), mean February rainfall (mm), mean annual solar radiation (kJ/day/m^2), mean annual temperature (°C), mean February temperature (°C), minimum temperature of the coldest month (°C, July), and October vapor pressure deficit (when persistent westerly winds result in strong geographic variation in vapor pressure deficit; Leathwick et al., 2003) (kPa). Present-day 100 m resolution climate surfaces were derived from observed meteorological data (1950–1980) fitted by thin-plate spline regression to a New Zealand digital elevation model (DEM) (Leathwick et al., 1998, 2003) using ANUSPLIN 4.1 (Hutchinson, 2000). These methods were used to fit observed meteorological data (1950–1980) to the LGM (c. 22,000 cal years BP) based on estimates of temperature depression from marine isotope stages and estimates of LGM topography obtained by extending the modern DEM down to the 120 m bathymetry (J.R. Leathwick, unpublished data). These climate data are held in a Geographic Information System (GIS) as ESRI (Environmental Systems Research Institute, Redlands, California) grids using New Zealand Map Grid (NZMG) coordinates.

Ecological niche models were generated with Maxent 3.3.1 (Phillips et al., 2006; Phillips and Dudík, 2008). A total of 173 localities for *E. lawsoni* and 167 for *P. bakewelli* (excluding Chatham Islands), including both sequenced and collection material, were used to build the models (Fig. 1b and c). Maximum iterations were increased to 2000, with other settings left at default values. To ensure consistency of model predictions among repeated runs, we performed a 10-fold cross-validation, in which a different 90% of localities were used to train the model and 10% were used to test it for each of 10 runs, such that each locality was used to test the model once. Data were projected onto LGM surfaces, using the 'fade by clamping' setting for output grids, to visually inspect for differences in regions projected as suitable habitat between replicate runs. Clamping grids were also inspected for differences in model output under different data partitions. The final geographical projections represent the mean point-wise strength of prediction over ten model runs.

Model performance was evaluated using threshold-dependent binomial omission tests and the Area Under the (Receiver Operating Characteristic; ROC) Curve (AUC) calculated by Maxent. Binomial omission tests utilize test data from each cross-validation run to generate *P*-values for 11 thresholds of occurrence (Liu et al., 2005; Phillips et al., 2006). The AUC varies along a continuous probability distribution between 0.5, indicating performance no better than random, to 1, indicating perfect assignment of presence, although in practice the maximum possible AUC is <1 (Phillips et al., 2006), and scores >0.75 are considered adequate for species distribution modeling applications (Pearce and Ferrier, 2000).

Critics have questioned the statistical independence of tests which use a single data set for both training and testing the resulting ENM (Raes and ter Steege, 2007; Phillips et al., 2009; Veloz, 2009). In the absence of independent test data, we incorporated a null model approach to test whether our models performed better than random without subdividing the original data. To build a null model for each species, we generated 99 sets of 173 (*E. lawsoni*) or 167 (*P. bakewelli*) localities, randomly drawn from areas of New Zealand with native forest cover based on Forest Service Mapping Series 6 (FSMS6) (Koordinates, 2008a,b), using Hawth's Tools

Fig. 1. New Zealand locations. (a) Regions for phylogeographic tests. Regions used for ancestral state reconstruction are in bold, and other locations are in regular type. Lines transecting both islands are boundaries for AMOVA hypotheses: thick light gray lines separate 5 biotic zones (Wardle, 1963), thin black line represents the Alpine Fault and thin dotted line represents the continental divide (after Hill et al., 2009), and thick dark gray lines are the southern and eastern extents of hypothesized LGM forest refugia (Alloway et al., 2007). (b) Locality data for *E. lawsoni* ENM. (c) Locality data for *P. bakewelli* ENM.

for ArcGIS. We then modeled all 99 randomly-drawn data sets, plus *E. lawsoni* or *P. bakewelli*, in Maxent without setting aside test data. All 100 AUCs were ranked, and species' AUCs within the top 5% were considered significantly different from random.

3. Results

3.1. Population genetics statistics

We obtained mitochondrial *cox1* sequence data from 168 *E. lawsoni* (843 bp) from 78 localities and 88 *P. bakewelli* (793 bp) from 53 localities (Supporting information; Genbank Accession nos. JF278627–JF278882). This discrepancy in sample size is related to collecting technique; *E. lawsoni* are more likely to be taken during substrate sifting, whereas *P. bakewelli* are largely hand-collected, which requires visually finding them in the field. Sequence and population statistics for *E. lawsoni* and *P. bakewelli* are given in Table 1. Tajima's *D* and Fu and Li's *F* and *D* were not significant for either species.

Of the 116 haplotypes sampled for *E. lawsoni*, none were detected at >3 localities, 102 were only recovered from one locality, and 84 were represented by a single individual. Mean pairwise genetic distance (base differences/sequence) was 15.77% (133 bp; corrected distance 0.7651 substitutions/site), while the maximum uncorrected pairwise genetic difference, between Kohuronaki (Northland) and Mt. Arthur (Nelson) was 24.56% (207 bp; corrected distance 1.8642 subs/site). The maximum within-population difference of 21.47% (181 bp; corrected distance 0.9644 subs/site) was detected at Akatarawa Saddle (Wellington). Nine

Table 2
Results of analysis of molecular variance (AMOVA) tests of *a priori* biogeographic hypotheses. Statistically significant *P*-values are indicated in bold. Population refers to individual localities, region refers to the division being tested, and *n* refers to the number of populations within regions, listed north to south (Fig. 1a).

Test	Source of variation	d.f.	Sum of squares	Variance components	% Variation	Significance tests
Epistranus lawsoni						
North Island vs.	Among regions	1	0.848	0.00137	0.28	**0.03238**
South Island	Pops w/in regions	76	51.656	0.16619	33.27	0
n = 36, 42	Within populations	86	28.55	0.33198	66.46	0
	Total	163	81.055	0.49954		
5 biotic zones	Among regions	4	3.615	0.00516	1.03	**0.00079**
(Wardle, 1963)	Pops w/in regions	73	48.89	0.16278	32.56	0
n = 18, 18, 20, 16, 6	Within populations	86	28.55	0.33198	66.41	0
	Total	163	81.055	0.49992		
North Island:	Among regions	1	0.695	0.0029	0.58	**0.0203**
2 biotic zones	Pops w/in regions	34	19.418	0.08537	17.08	0
n = 18, 18	Within populations	32	13.167	0.41146	82.34	0
	Total	67	33.279	0.49973		
South Island:	Among regions	2	2.072	0.00653	1.3	**0.02307**
3 biotic zones	Pops w/in regions	39	29.472	0.20894	41.76	0
n = 20, 16, 6	Within populations	54	15.383	0.28488	56.94	0
	Total	95	46.927	0.50034		
South Island:	Among regions	1	1.072	0.00432	0.86	**0.00436**
Southern Alps	Pops w/in regions	40	30.471	0.21079	42.16	0
n = 20, 22	Within populations	54	15.383	0.28488	56.98	0
	Total	95	46.927	0.5		
LGM refugia	Among regions	1	0.762	0.00042	0.08	0.34822
(Alloway et al., 2007)	Pops w/in regions	76	51.743	0.16671	33.4	0
n = 19, 59	Within populations	86	28.55	0.33198	66.51	0
	Total	163	81.055	0.49911		
Pristoderus bakewelli						
North Island vs.	Among regions	1	0.626	0.00153	0.31	0.12347
South Island	Pops w/in regions	49	26.814	0.07672	15.35	0
n = 17, 34	Within populations	33	13.917	0.42172	84.35	0
	Total	83	41.357	0.49997		
5 biotic zones	Among regions	4	2.416	0.00243	0.49	0.11782
(Wardle, 1963)	Pops w/in regions	46	25.025	0.07568	15.14	0
n = 6, 11, 24, 6, 4	Within populations	33	13.917	0.42172	84.37	0
	Total	83	41.357	0.49982		
Upper South vs.	Among regions	1	0.601	0.00174	0.35	0.24168
Lower North Is.	Pops w/in regions	33	18.075	0.08099	16.22	0
n = 11, 24	Within populations	22	9.167	0.41667	83.43	0
	Total	56	27.842	0.49939		
South Island:	Among regions	1	0.652	0.00357	0.71	0.05366
Southern Alps	Pops w/in regions	32	17.524	0.0764	15.27	0
n = 14, 20	Within populations	23	9.667	0.42029	84.02	0
	Total	56	27.842	0.50025		

localities, from the North and South Islands, had average within-population differences of zero. A Mantel test for matrix correlation between genetic distance (FST) and log-linear geographic distance was significant ($P = 0.0374$, $r = 0.1126$), but explained only a limited amount of variation in the data ($r^2 = 0.0127$).

For *P. bakewelli*, none of the sampled 77 haplotypes were shared by >2 localities, 72 were detected at only one locality, and 67 were represented by a single individual. Mean pairwise genetic distance (base differences/sequence) was 9.71% (77 bp; corrected distance 0.2381 subs/site), while the maximum 14.88% (118 bp; corrected distance 0.5712 subs/site) was detected between Waetewaewae Track (Wellington) and Pigeon Saddle (Nelson). The highest average within-population difference, 13.24% (105 bp; corrected distance 0.3987 subs/site), was detected from the Speargrass Track (Buller). Three of the four localities with average within-population differences of zero were from the South Island. Mantel tests for isolation by distance, including and excluding the Chatham Islands, were not significant.

Analysis of molecular variance indicated that the majority of molecular variation was within, rather than between, populations. For *E. lawsoni*, the tests of North vs. South Island, five biotic zones, two North Island zones, three South Island zones and spanning the Southern Alps were all statistically significant (Table 2), but variation among the regions being compared accounted for less than 1.5% of the total. Over 50% of molecular variation in *E. lawsoni* was detected within populations. Hypothesized LGM refugia did not explain a statistically significant portion of the variation in *E. lawsoni*, and none of the tests with *P. bakewelli* yielded significant results.

3.2. Phylogenetic relationships

For both species, the marginal posterior distribution of the exponential growth rate parameter included zero, suggesting the data were more compatible with the constant size population model. For *E. lawsoni*, most of the marginal density was less than zero (mean = −0.0509, 95% posterior credibility interval of −0.112 to 0.005), suggesting population size has remained constant or declined during much of the time measured by the genealogy. However, tree topologies and node support values were nearly identical between the constant size and exponential growth models for both species, regardless of whether the strict or relaxed

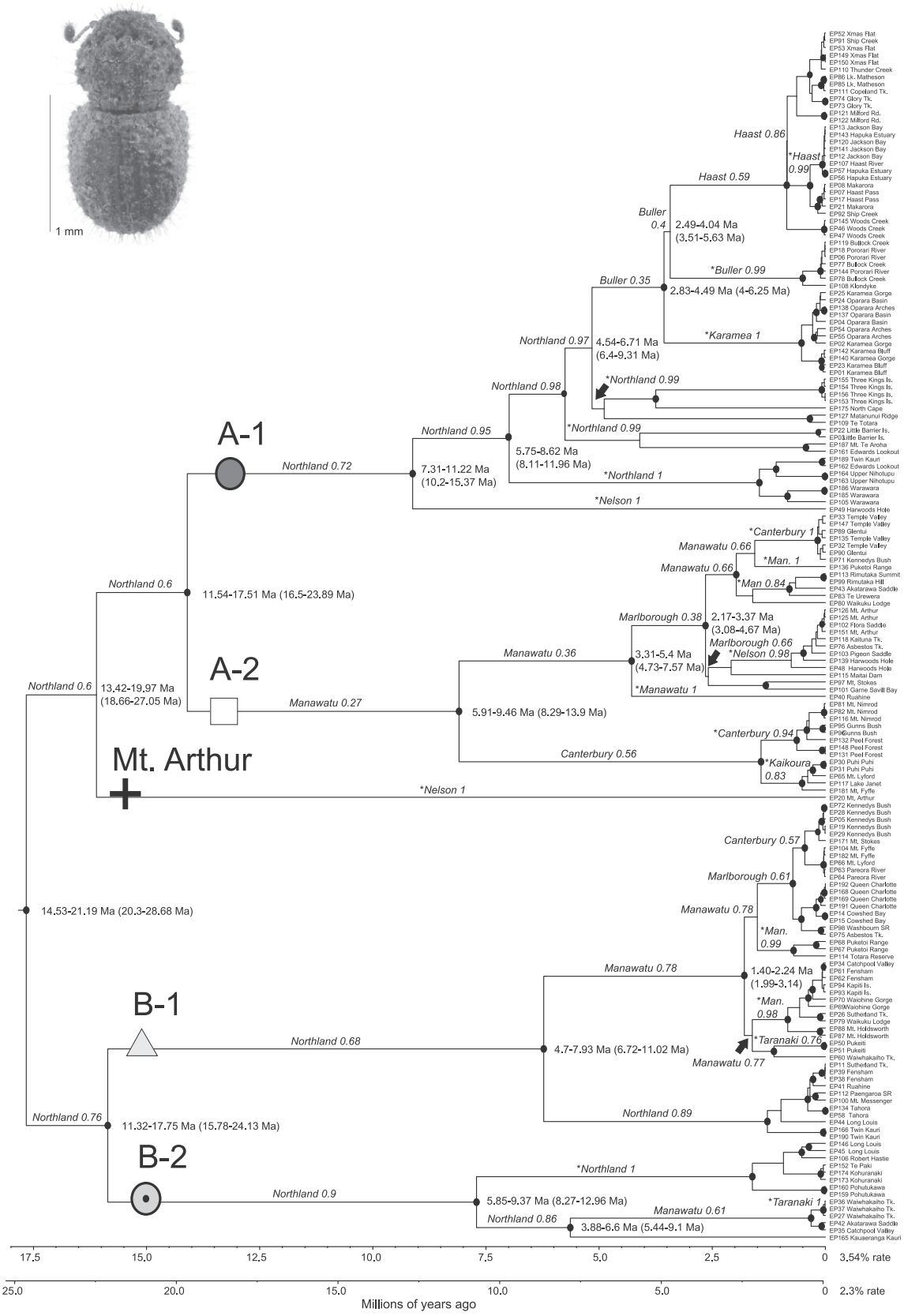

Fig. 2. Bayesian coalescent tree for *Epistranus lawsoni* (strict clock, 3.54% My^{-1} rate), with branch lengths drawn proportional to time. Date estimates (95% credibility interval) calculated using both substitution rates are given at nodes, with dates from the slower rate in parentheses, excluding at tree tips. Black dots indicate all nodes with posterior probabilities >0.95. The highest-scoring region-state and its state probability is indicated above each branch, excluding at tree tips, and * indicates that all descendent branches share the same state. Photograph by B. Rhode, Landcare Research.

clock was used. Posterior probabilities (pp) shown, unless stated, were generated under the constant size, 3.54% My^{-1} rate models.

For *E. lawsoni*, Bayesian coalescent analyses yielded a tree with well-resolved deep nodes (Fig. 2), with the exception of a single long-branch lineage from Mt. Arthur (Nelson), in the South Island, which connects to Clade A near the root (pp = 0.5578). Clade A spans the length of the North and South Islands. Within Clade A are A-1, which extends along the South Island's west coast and from the central to northern North Island, including the Three Kings Islands, and A-2, which includes the southern North Island and the east coast, Nelson and Marlborough regions of the South Island (pp = 0.9957). The remaining lineages form Clade B, in which B-1 spans the entire North Island and eastern South Island and B-2 is restricted to the North Island (pp = 0.9932). Key geographic features of the *E. lawsoni* tree include paraphyletic relationships between the North and South Islands and the apparent distribution of subclades consistent with known geographic boundaries: the Southern Alps and Alpine Fault, dividing the South Island longitudinally, and the Taupo Line (e.g., Wardle, 1963, Fig. 3a; see discussion), transecting the central North Island.

Coalescent analyses also yielded a well-resolved tree for *P. bakewelli* (Fig. 4), with the exception of Clade C, which contains the only sequences from the southern South Island. Attachment of the root is between Clades C–D and the remainder of the tree (Clades E–G) (pp = 1). Clade C attaches to D, which is distributed the length of the North Island to Marlborough in the South Island, near the root (pp = 0.5201). Within Clade D, D-1 is restricted below the Taupo Line but extends southward into Marlborough, while D-2 includes the entire North Island. These subclades form a monophyletic group (pp 1). Clade E (pp = 0.9999) is restricted to Karamea localities, while Clade F includes the southern North Island, northern South Island, and Canterbury, and Clade G covers the South Island's west coast and extends east into Marlborough (F–G pp = 0.9325). Key geographic features for *P. bakewelli* are similar to those for *E. lawsoni*: the South Island's west coast (south of Nelson) is represented by a single clade, and two lineages in the lower North Island are delimited by the Taupo Line (Fig. 3b).

3.3. Coalescent phylogeographic reconstruction

Ancestral spatial reconstruction puts the root for *E. lawsoni* in Northland with a state probability (sp) of 0.63, with the next most probable location as Manawatu (sp = 0.14). When state probabilities for all regions are ranked, regions south of Nelson and Marlborough fall into the lowest 5% and can be ruled out as potential root locations. Coalescence of Mt. Arthur with Clade A, Clades A-1 and A-2, and B-1 and B-2 are also placed in Northland (sp = 0.60, sp = 0.60 and sp = 0.76, respectively). South Island lineages in A-1 (west coast), as well as the Mt. Arthur lineage, are hypothesized as descending directly from Northland ancestors, while those in A-2 and B-1 (northern and east coast) descended from Manawatu. The two Southland localities in Clade A-1 are most closely related to those from Haast Pass (sp = 0.85 and sp = 0.91), but the region-state of the most recent common ancestor all of the west coast and southern South Island populations, after divergence from the Northland region-state, was poorly resolved (Buller, sp = 0.35;

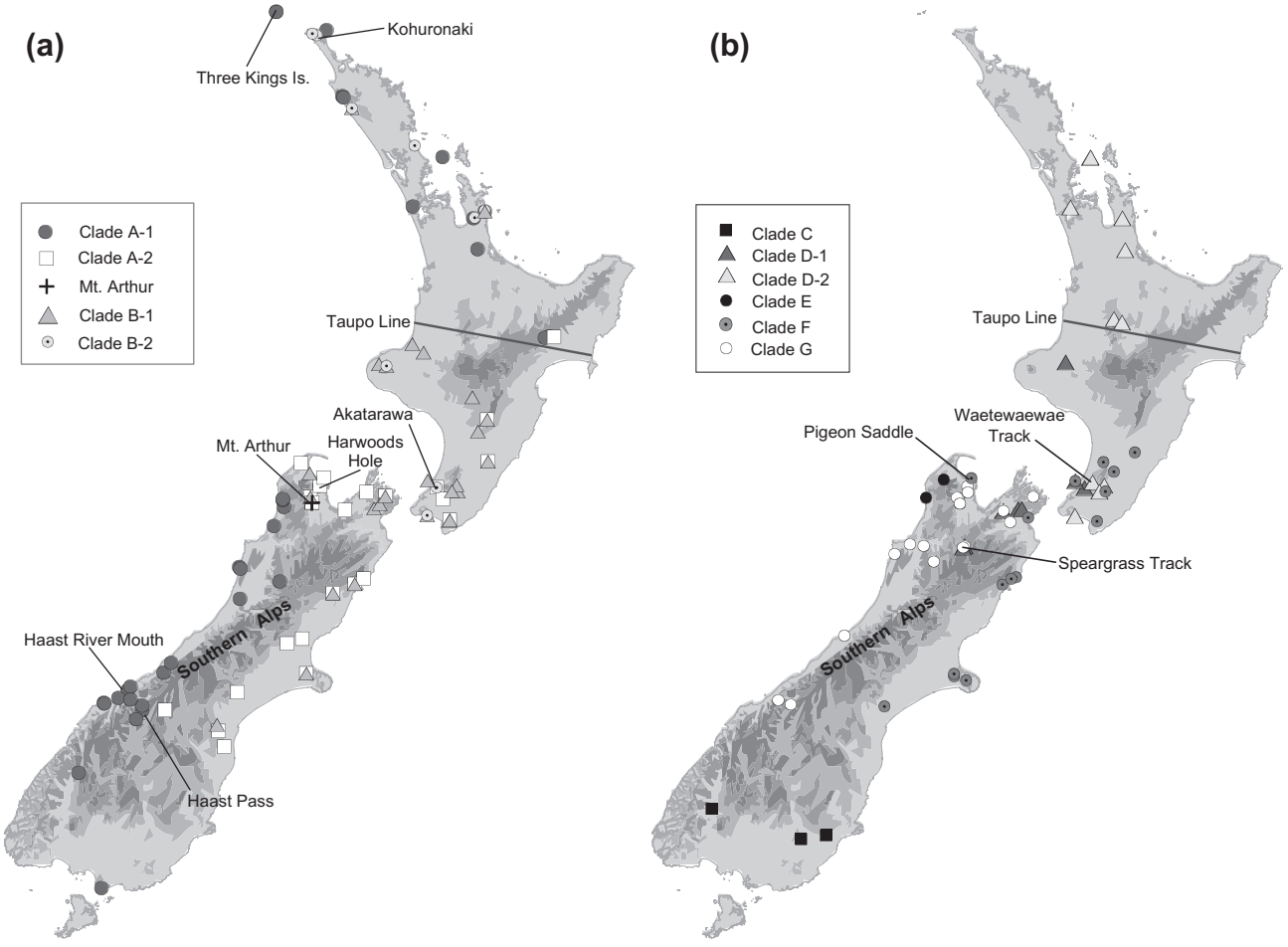

Fig. 3. Distribution of populations sampled for molecular analysis. Labels indicate specific localities mentioned in the text. Map shading indicates topographic relief. Taupo Line is after Wardle (1963). (a) *Epistranus lawsoni* sample locations, with clade symbols after Fig. 2. (b) *Pristoderus bakewelli* sample locations, with clade symbols after Fig. 4 (Chatham Islands not shown).

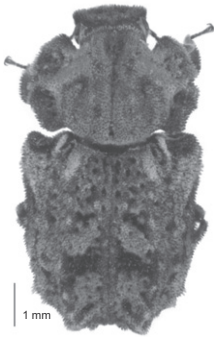

Fig. 4. Bayesian coalescent tree for *Pristoderus bakewelli* (strict clock, 3.54% My^{-1} rate), with branch lengths drawn proportional to time. Date estimates (95% credibility interval) calculated using both substitution rates are given at nodes, with dates from the slower rate in parentheses, excluding at tree tips. Black dots indicate all nodes with posterior probabilities >0.95. The highest-scoring region-state and its state probability is indicated above each branch, excluding at tree tips, and * indicates that all descendent branches share the same state. Photograph by B. Rhode, Landcare Research.

Haast, sp = 0.19; Karamea, sp = 0.17; Southland, sp = 0.12). Nelson populations in Clades A-2 and B-1 descended from Marlborough (sp = 0.55 and sp = 0.77, respectively), rather than from any of the western populations. In the North Island, Taranaki populations descended from Manawatu, not Northland.

Root placement for *P. bakewelli* is poorly resolved, with the highest state probabilities for Manawatu (sp = 0.24), Nelson (sp = 0.18), Marlborough (sp = 0.15) and Buller (sp = 0.12). While the other deep nodes are also poorly resolved, it is likely that Clades E, F and G arose in the South Island, as those nodes have multiple South Island regions with state probability >0.2, compared to North Island regions with state probability <0.05. All nodes indicating coalescence of South Island regions show little support for individual region-states (sp < 0.5) except at the tree tips, with Buller populations descending from Marlborough ancestors in both clades where Buller sequences appear (D-1, sp = 0.84; G, sp = 0.37). For the Southland and Chatham Islands lineages (Clade C), Manawatu (sp = 0.27), Nelson (sp = 0.17), Marlborough (sp = 0.13) and Buller (sp = 0.11), had the four highest ancestral state probabilities, clearly implicating neither a North Island nor South Island origin. Lineages apparently originating in the North Island (Clade D) received much stronger support, with each node within Clade D assigned a region with state probability >0.5.

Bayes factor analyses of rates of geographic state transition resulted in some regions with limited or no connections for both species (Fig. 5). For *E. lawsoni*, the highest Bayes factors (and best supported dispersal pathways) were between the adjacent Taranaki and Manawatu, Canterbury-Kaikoura, and Haast-Southland (Fig. 5a, Table 3). No significant rates of state transition were indicated between east and west coast populations in the South Island, suggesting that little, if any, dispersal occurs between these regions. For *P. bakewelli*, Canterbury and Southland were not connected to any other regions in mainland New Zealand, reflecting the low posterior support (pp = 0.5201) for the attachment of Southland/Chatham Islands (Clade C) to Clade D. Aside from the Chatham Islands, migratory pathways within *P. bakewelli* are over relatively short distances, with the highest Bayes factors between Nelson-Buller and Northland-Manawatu (Fig. 5b).

3.4. Molecular clock

Dates estimated under the strict and relaxed clocks (2.3% My^{-1} rate) were strongly concordant for *E. lawsoni*, with all estimates for coalescent dates within 1 Ma of each other (typically less than 0.5 Ma apart), and with 95% posterior credibility intervals of similar breadth (data not shown). Coalescence at the root was estimated at 17.83 or 24.37 Ma using the faster and slower rates, respectively, a difference of nearly 7 Ma (95% posterior credibility intervals shown in Fig. 2). Separation of the Mt. Arthur lineage from Clade A was estimated at 16.67 or 22.87 Ma. Divergence of A-1 from A-2 and B-1 from B-2 were nearly simultaneous, estimated at 14.42 or 19.90 Ma and 14.43 or 19.87 Ma, respectively, a difference of over 5 Ma between clock rates. Within clades, coalescence of monophyletic South Island lineages with North Island branches occurred at 5.61 or 7.99 Ma in A-1 and 1.81 or 2.55 Ma in B-1.

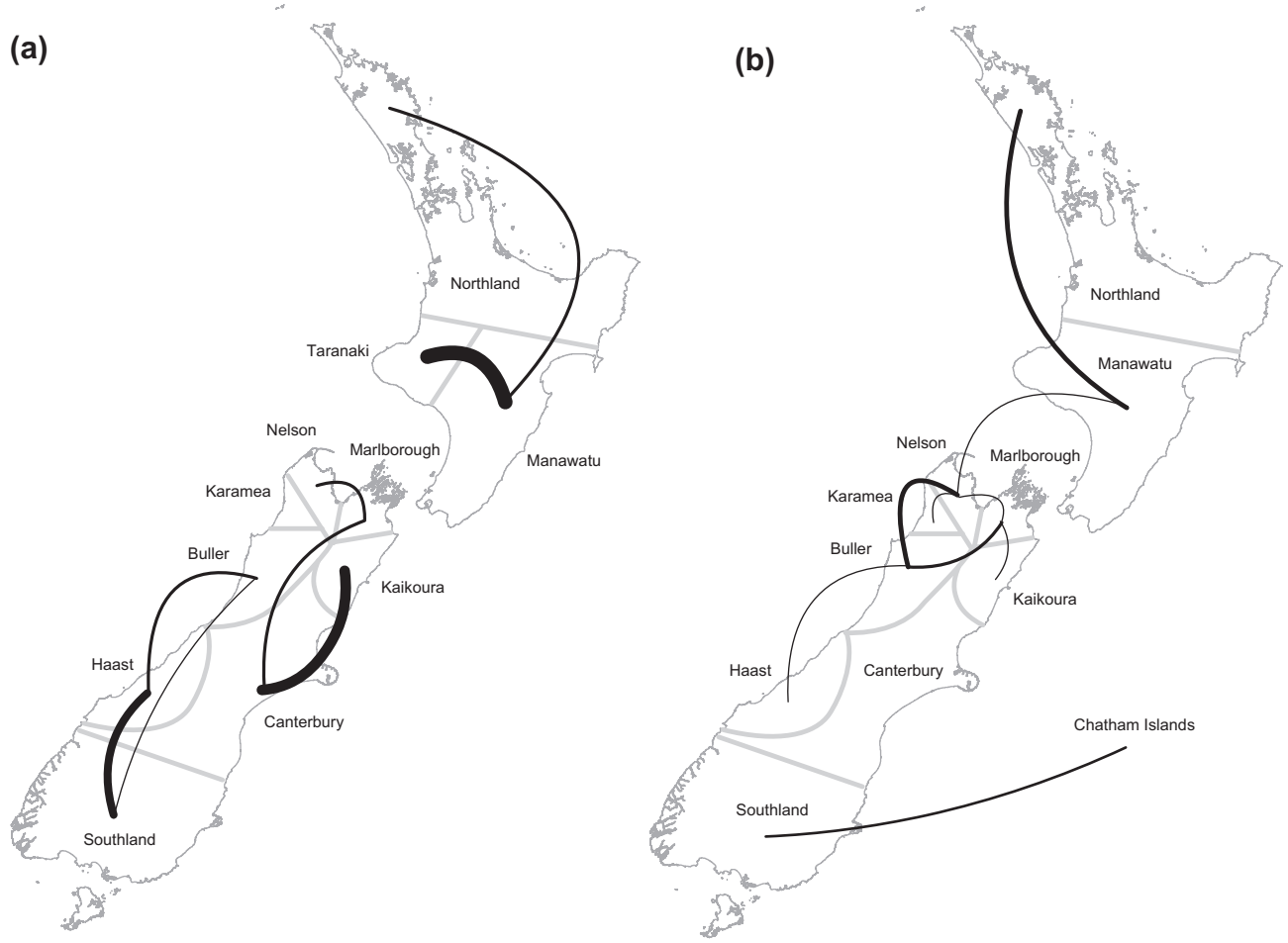

Fig. 5. Bayes factor tests for significant (BF > 3.0) rates of transition between geographic states, indicating a gene flow matrix. Line thickness indicates the relative strength by which the rates are supported. (a) Gene flow matrix for *E. lawsoni*. (b) Gene flow matrix for *P. bakewelli*.

Table 3
Bayes factor tests for significant (BF > 3.0) rates of transition between geographic states.

Species	Bayes factor	Regions
Epistranus lawsoni	7265.6	Manawatu × Taranaki
Epistranus lawsoni	3868.5	Canterbury × Kaikoura
Epistranus lawsoni	677.4	Haast × Southland
Epistranus lawsoni	48.1	Canterbury × Marlborough
Epistranus lawsoni	46.9	Nelson × Marlborough
Epistranus lawsoni	28.8	Manawatu × Northland
Epistranus lawsoni	15.0	Buller × Haast
Epistranus lawsoni	6.1	Marlborough × Manawatu
Epistranus lawsoni	5.6	Karamea × Buller
Epistranus lawsoni	3.6	Buller × Southland
Pristoderus bakewelli	261.1	Nelson × Buller
Pristoderus bakewelli	158.0	Manawatu × Northland
Pristoderus bakewelli	60.7	Southland × Chatham Is.
Pristoderus bakewelli	52.7	Buller × Marlborough
Pristoderus bakewelli	15.7	Buller × Haast
Pristoderus bakewelli	10.1	Nelson × Manawatu
Pristoderus bakewelli	8.2	Kaikoura × Marlborough
Pristoderus bakewelli	7.8	Nelson × Karamea
Pristoderus bakewelli	5.0	Nelson × Marlborough

For *P. bakewelli*, coalescent results were also strongly concordant between the strict and relaxed clocks (2.3% My^{-1} rate), with nearly identical estimates for both coalescent dates and 95% posterior credibility intervals (data not shown). Coalescence at the root was estimated at 6.81 or 9.58 Ma using the faster and slower rates, respectively (95% posterior credibility intervals shown in Fig. 4). Coalescence between Clades C (southern South Island) and D (North Island and southern South Island) was estimated at 6.13 or 8.65 Ma. Divergence of North and most South Island lineages within Clades D-1 and F occurred at 2.42 or 3.44 Ma and 3.09 or 4.37 Ma, respectively, although lineages from Pigeon Saddle (Nelson) in Clade F diverged from the North Island more recently. The Canterbury lineages diverged from the rest of Clade F at approximately 3.91 or 5.57 Ma, and colonization of the Chatham Islands from the southern South Island was estimated at 1.05 or 1.49 Ma.

3.5. Ecological niche modeling

Bioclimatic models of the distribution of *E. lawsoni* performed significantly better than random. The 10-fold cross-validation runs yielded an average AUC of 0.817 (sd 0.033, range 0.7742–0.8736) and performed significantly better than random across all thresholds and runs except for one instance of $P = 0.56$ at the lowest measured threshold for one run. Heuristic estimation of relative contributions of the environmental variables to the Maxent model ranked them as follows: annual temperature (19.8%), February rainfall (19.1%), annual rainfall (16.3%), February temperature (12.6%), minimum temperature (12.3%), October vapor pressure deficit (10.7%) and solar radiation (9.2%). Almost no "clamping", where environmental variables are restricted to the range of values encountered during training after being detected outside of that

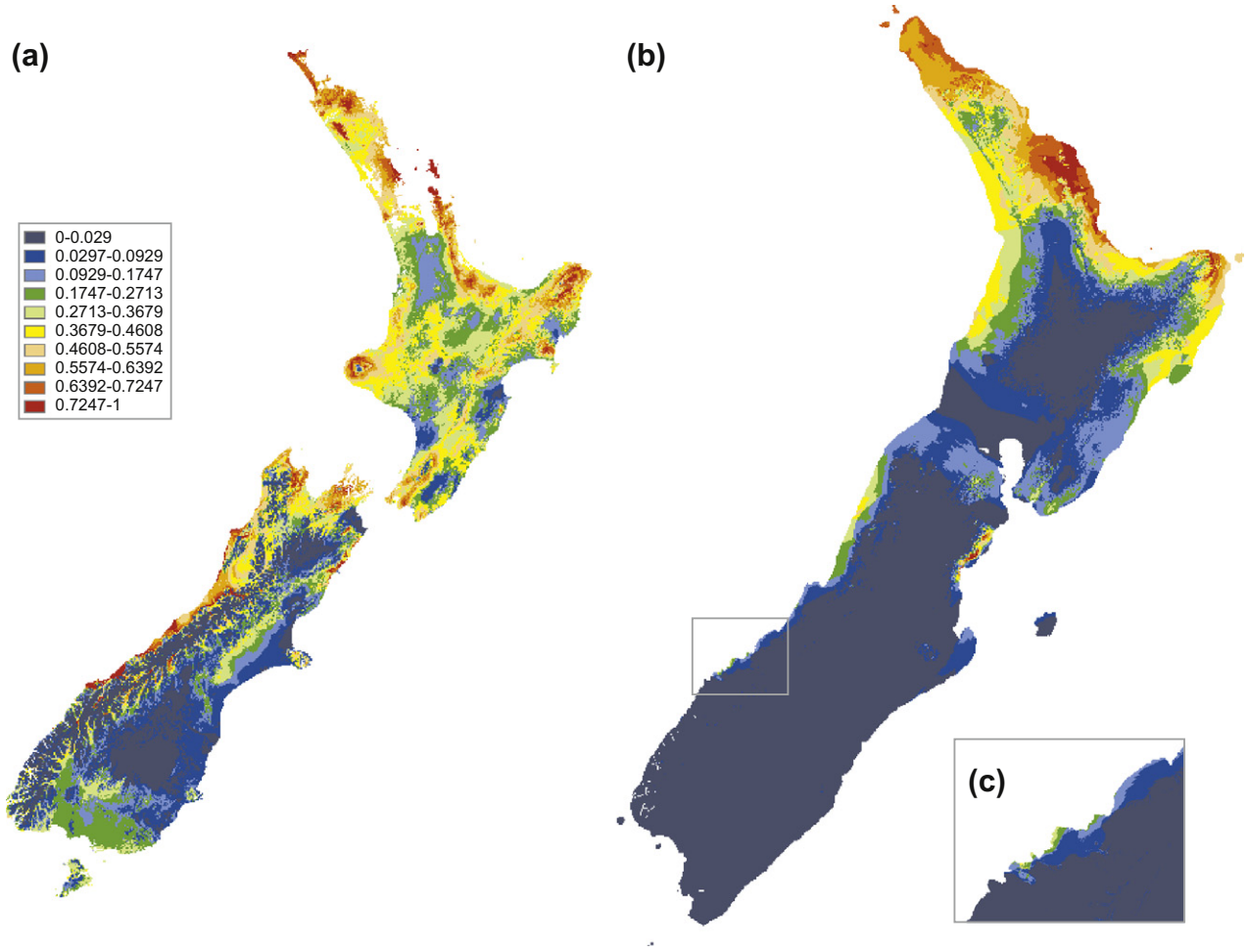

Fig. 6. Ecological niche models for *Epistranus lawsoni*. Warmer colors more suitable habitat, averaged across 10 cross-validation runs. (a) Current distribution. (b) LGM distribution. (c) LGM detail: Haast River mouth.

range during testing, was detected during projection onto LGM surfaces. In the null model tests, the AUC score for *E. lawsoni* (0.861) ranked within the top 5% against models drawn randomly from forests (AUC range 0.7956–0.8679).

Under current climate conditions, *E. lawsoni* was projected to be widely distributed throughout the North Island (Fig. 6a). In the South Island, less suitable conditions were projected in montane areas and much of the southeast. Under LGM climate conditions (c. 22,000 cal years BP) most of the South Island except the northeast and northwest coasts at Kaikoura and Karamea were projected as less suitable for *E. lawsoni*, although smaller refugia were projected along the southwest coast near Haast River and in the Marlborough Sounds with lower probability (Fig. 6b and c). These four locations were indicated in all 10 repeated runs. Suitable conditions were projected nearly continuously along both coasts in the northern two-thirds of the North Island, potentially with outlying refugia in Wellington and Wairarapa, spanning an area which—then and now—was indicated as less suitable for *E. lawsoni*.

Results for *P. bakewelli* scored lower and were more variable between runs than *E. lawsoni*. The 10-fold cross-validation runs yielded an average AUC of 0.738 (sd 0.061, range 0.6275–0.8395), and results of the binomial omission tests were not significant at a variety of thresholds. When its distribution was projected onto LGM surfaces, treatment of the southern North and South Islands was extremely variable between individual runs, indicating that the way the data were partitioned had a large impact on how the environmental variables fit, and clamping was detected over large areas. In the null model test, the AUC score for *P. bakewelli* (0.815) ranked lower than all but four models randomly drawn from forests (AUC range 0.7964–0.8688). Since models were not significantly different from random predictions, no projections are presented for *P. bakewelli*.

4. Discussion

Interpreting phylogeographic patterns for *E. lawsoni* and *P. bakewelli* in light of New Zealand's turbulent history of landscape evolution is challenging even with the data now at hand. High genetic diversity and ancient coalescent dates are difficult to reconcile with the late-Pleistocene ENM for *E. lawsoni*, there is no ENM with which to compare ambiguous geographical relationships for *P. bakewelli*, and different coalescent time scales between species confuses the apparent similarity of phylogenetic breaks over geographic space. This poses a critical question: how do we choose between apparently conflicting phylogenetic and ENM results? Here we address this challenge, identify areas of concordance among methods, and hypothesize a broad phylogeographic scenario for both species in light of the LGM and earlier events.

4.1. Genetic diversity, vicariance and dispersal

One of the most striking features of the genetic data is the remarkably high levels of intraspecific variation, particularly for *E. lawsoni*. This is not unprecedented for non-vagile litter-dwelling species; Boyer et al. (2007) detected an average pairwise difference of 14.4% in the New Zealand mite-harvestman *Aoraki denticulata* (Forster), compared to 15.8% for *E. lawsoni* and 9.71% for *P. bakewelli*. All three species are flightless, and *E. lawsoni* adults are <2 mm in length, suggesting that high genetic diversity and geographic structuring are at least partly related to poor dispersal capabilities (e.g., Boyer et al., 2007). The genitalia of the two species of zopherids are conserved, though the spiculum gastrale of *E. lawsoni* exhibits minor variation that is not consistent with geographic distribution or the *cox1* topology. The size range and cuticular morphology of *P. bakewelli* is extraordinary, but apart from the concentration some of the larger individuals from the Nelson and West Coast areas, morphology does not correspond with geography and *cox1* topology (R. Leschen & K. Marske, unpublished). Therefore, based on the data currently available, we continue to treat *E. lawsoni* and *P. bakewelli* as individual species rather than species complexes.

Intense population structuring over a limited spatial extent appears to be a recurrent pattern of the leaf and log litter fauna (e.g., Garrick et al., 2004). High intraspecific genetic variation has been repeatedly detected in terrestrial snails, with maximum mtDNA divergences of 12–15% in the slowly-evolving 16s gene (e.g., Thomaz et al., 1996; Watanabe and Chiba, 2001) and *cox1* (Hugall et al., 2002), and in at least one case, extensive morphological variation was also observed (Thomaz et al., 1996). High intraspecific variation (17.2%, *cox1*) was also detected in Antarctic springtails *Friesia grisea* (Schäffer), for which no obvious morphological characters denote separate species (Torricelli et al., 2010), while Garrick et al. (2004) detected divergences up to 11.4% (corrected) in giant springtails from the Australian Tallaganda (Garrick et al., 2004). This and other Tallaganda studies suggest that strong genetic differentiation over a fine spatial scale is likely the rule, rather than the exception, for non-vagile members of the litter fauna in complex landscapes (e.g., Sunnucks et al., 2006).

Much of the genetic diversity in the zopherids is within, rather than between, populations. Although the AMOVA results may be affected by low intra-population sample sizes, for *E. lawsoni*, the mean intra-population difference is only 3.86%, but the maximum difference is 21.47%. Where members of a population belong to either Clade A or Clade B, observed substitutions among sequences are typically $\leqslant$10 bp, with some exceptions, but at localities where A and B are sympatric, members of the same population are typically separated by >100 (>12%) base pair differences. This contrasts with the findings of Boyer et al. (2007), in which variation was higher between populations, but is similar to observations for terrestrial snails, with some co-occurring haplotypes differing by >10% (Watanabe and Chiba, 2001). Individual snails tend to have small local ranges despite the tendency of snail species to rapidly colonize vacant habitats (Davison, 2000), with limited gene flow and repeated vicariance and dispersal of populations through time resulting in fine-scale geographic variation, and expansion and migration from different areas resulting in the mixture of distantly-related lineages within some populations (Watanabe and Chiba, 2001). A similar pattern is likely the case for *E. lawsoni*, where a relatively old species has persisted in a rapidly evolving landscape and is currently widely distributed through New Zealand and several offshore islands. This is a different dynamic than in *A. denticulata*, where the species' distribution is restricted to a part of the South Island believed to harbor glacial refugia, suggesting long-term vicariance without extensive dispersal (Boyer et al., 2007).

4.2. Molecular clock: ancient clades or misleading rates?

High genetic diversity contributes to the second notable feature of the genetic results: ancient coalescent dates, particularly for *E. lawsoni*. This necessitates a cautious interpretation of the molecular clock, as we are unable to reject the possibility of an accelerated substitution rate (e.g., Boyer et al., 2007) or time-dependent mutation rates (e.g., Ho et al., 2007), both of which would inflate divergence estimates. We indirectly examined the potential influence of time-dependent mutation rates through the use of a relaxed clock, and observed very little difference in either estimated divergence dates or posterior credibility intervals when compared to strict clock estimates. We also used a normal prior with a 10% standard deviation on clock rate in the strict clock analyses, allowing some rate variation over the tree. However, no external calibration data exist for either species, and so while Papadopoulou et al.'s (2010)

faster rate of 3.54% My^{-1} is likely more appropriate than Brower's (1994) slower rate of 2.3% My^{-1}, as it was calibrated for flightless beetles, we are unable to explicitly test whether our data conform to either rate. Therefore, we are able to relate our results to New Zealand's geological history in only the broadest sense.

Mitochondrial DNA is no longer assumed to be selectively neutral (Zink and Barrowclough, 2008; Galtier et al., 2009), and although we tested for selection and could not reject the null hypothesis of neutrality, phylogeographic structuring can occasionally obscure the signature of selection (Rosenberg and Norborg, 2002). This is particularly true for balancing selection, which results in deep divergences among haplotypes—although each divergent haplotype tends to be repeated within its local population, with deep coalescence between populations (e.g., Charlat et al., 2009), which is not the case for *E. lawsoni*.

Coalescent analyses are often regarded as superior to using a single topology for estimating a species' evolutionary history because they account for stochastic evolutionary processes within lineages (Hickerson et al., 2010). However, phylogeographic structuring can lead to the overestimation of divergence dates (Edwards and Beerli, 2000), with subdivided populations with low migration rates experiencing significantly deeper coalescence than panmictic populations (Edwards and Beerli, 2000; Jesus et al., 2006). This problem is particularly acute when a population reaches reciprocal monophyly, resulting in broader posterior credibility intervals for coalescent dates, especially when a single locus, such as *cox1*, is used (Edwards and Beerli, 2000), and for *E. lawsoni*, in which Clades A and B are reciprocally monophyletic, extremely large posterior credibility intervals (~8–10 Ma using the slower rate) were estimated on the deeper nodes. In this scenario of highly geographically structured populations, collecting gaps, under-sampling within populations and overall decline in population size (as indicated by the negative exponential growth rate for *E. lawsoni*) might all be expected to exacerbate date overestimation by increasing the time to the most recent common ancestor (Jesus et al., 2006).

That *E. lawsoni* is currently distributed throughout New Zealand, yet was projected to have a greatly reduced range only 22,000 years ago (Fig. 6b and c), seems at odds with the long-term population isolation and vicariance implied by the ancient divergence dates. However, coalescent ancestral state reconstruction places the root and several of the deeper nodes (Clades A, B and Mt. Arthur) in Northland, the part of the modern North Island most likely to have been emergent during the Oligocene high sea stand at ~23 Ma (Bunce et al., 2009), and indicates that all modern South Island populations descended from North Island ancestors, with the majority diverging less than ~6–8 Ma. This divergence estimate is consistent with the narrowing of the Manawatu Strait separating the proto-North and South Islands at ~6 Ma (Bunce et al., 2009). Posterior credibility intervals narrow closer to the tree tips, and while they only reduce to a few hundred thousand years—not enough to specifically implicate late Pleistocene processes—most of the phylogeographic evolution of this species is estimated to have occurred within the last 10 Ma, during which New Zealand experienced extensive geographical reorganization and topographic development (Walcott, 1979; King, 2000; Pulford and Stern, 2004).

For *P. bakewelli*, the coalescent dating issues described above may be amplified by the lower sample size, increased number of populations represented by a single specimen, and reciprocal monophyly at the root. However, these coalescent dates are also consistent with known geological events, with root coalescence <12 Ma between lineages on either side of the narrowing Manawatu Strait, and near-simultaneous divergences of Clades D-1 and D-2 and E, F and G (3–8 Ma) consistent with uplift of mountain ranges on the South Island. While this convenient congruence between estimated dates and geological events does not entirely dispel the risk associated with strict interpretation of the date estimates, it suggests that they may be accurate enough to use as starting points for addressing the evolutionary histories of these species.

4.3. Ecological niche models and glacial refugia

The ENM for *P. bakewelli* demonstrated consistent poor fit between predictor variables and model performance and was not significantly different from models based on a generalized forest distribution. This suggests that the niche of *P. bakewelli* may be determined primarily by variables other than those tested (e.g., non-climatic variables), or that collection bias (visiting primarily native forest) in the distribution data is stronger than the measured climate trends. Failure of the ENM combined with poor coalescent resolution of historical connections between South Island regions (possibly due to low genetic sample sizes) makes predictions about LGM refugia locations tenuous.

The ENM for *E. lawsoni* was statistically robust, and was consistent with the phylogenetic results, with the eastern and western South Island represented by different lineages, but was difficult to reconcile with the coalescent dates, in which even nodes near the tips have divergence dates ranging into the hundreds of thousands of years. Given the poor dispersal ability inferred for this species, deep divergences may also suggest the presence of cryptic microrefugia, which occur in sheltered locations that vary from regional climate patterns and are therefore undetectable using our elevation-scaled climate grids (Ashcroft, 2010). Such microrefugia have been invoked to explain the deep divergences and fine-scale geographic structuring of the Tallaganda fauna (Garrick et al., 2004; Sunnucks et al., 2006). The spatial distribution of lineages for *E. lawsoni* does not appear to implicate microrefugia outside of those projected by the ENM (unless we consider *every* sampled population as originating in a separate refugium), and the deep genetic lineages may be the result of preservation in the same refugia through multiple glacial cycles.

Congruence between phylogeographic patterns and the ENM for the South Island may have resulted from Pleistocene glacial refugia or an earlier event such as mountain orogeny, which would have partitioned existing lineages into similar patterns. These explanations are not mutually exclusive, and the projected coastal refugia may have preserved and amplified the genetic signal of vicariance on either side of the rising Southern Alps. A decline in effective population size during this period of increased fragmentation would further enhance population structuring, driving deeper coalescence between lineages. However, without more apparent temporal overlap between the ENM and phylogeny, neither can be used to explicitly test the other, and both must remain as independent hypotheses. Projected refugia for *E. lawsoni* are similar to those for *Agyrtodes labralis* (Broun) (Leiodidae), another saproxylic mycophagous beetle (Marske et al., 2009), and the Kaikoura refugium may have been shared by the stick insect *Argosarchus horridus* (White) (Buckley et al., 2009), but we cannot use the genetic data to evaluate whether *E. lawsoni* utilized these refugia without being able to relate the two methodologies in a less qualitative fashion.

4.4. Phylogeography on a changing archipelago

A variety of methodological developments have expanded coalescent theory to transform phylogeography from a *post hoc* interpretive discipline into a rigorous statistical study (Hickerson et al., 2010). These methods have taken the form of either explicit hypothesis testing through data simulation (e.g., Carstens and Richards, 2007; Mardulyn et al., 2009) or inference of historical dispersal patterns through ancestral state reconstruction (e.g., Lemey et al., 2009). Both have their limitations: in the former, hypotheses are based on *a priori* knowledge of the study area (e.g., geological events, such as mountain orogeny) and are difficult to apply in a

continuous landscape with multiple potential vicariant boundaries, particularly with the low level of dating precision afforded by a single locus. In the latter, as implemented here, the geographic priors on rates of state transition are uninformative, with geographic relationships estimated from the sequence data alone, and geographic reconstructions are less certain at deeper nodes even where the coalescent topology is well-resolved. For this study, broad posterior credibility intervals on lineage coalescences, combined with the calibration issues described above, discouraged the use of hypothesis testing via simulation, which requires *a priori* incorporation of several coalescent population parameters. However, particularly in the case of *E. lawsoni*, the combination of gene flow matrices and estimation of region-states for most nodes allowed differentiation between spatial seeding of an area (e.g., dispersal between Northland and Mt. Arthur) and sustained gene flow among regions.

For *E. lawsoni*, the gene flow matrix indicated two separate dispersal networks, with little to no gene flow between South Island west coast and east coast + North Island populations. This suggests that the Southern Alps are a significant barrier to gene flow in this species, and that lineages in separate refugia on the east and west coast were separated prior to the last glaciation. On the west coast, dispersal pathways with the strongest Bayes factors were those connecting Haast to Southland and Buller, suggesting the potential importance of this small coastal refugium relative to the larger one projected for Karamea. Connection between Kaikoura and Canterbury suggests that this potential refugium likely seeded the east coast, but with diffusion between the North and South Islands contributing additional haplotypes. For *P. bakewelli*, the gene flow matrix did not illuminate the origin of the eastern and southern South Island haplotypes, but the network of connections on and extending from the northwest coast suggest the possible presence of a refugium similar to that projected for *E. lawsoni*. Dispersal pathways are restricted to regions within close proximity to each other, with steady population expansion rather than long distance dispersal as the predominate driver of gene flow.

Phylogenies of both species share broad geographical patterns, including a north–south division concordant with the Taupo Line on the North Island and an east–west division roughly concordant with the Southern Alps and Alpine Fault on the South Island. Similar patterns do not necessarily implicate similar drivers of these patterns, particularly given the differences in divergence estimates and migratory pathways. In the North Island, the Taupo Line provides a well-established boundary in distributions of many taxa, although its exact location varies (Rogers, 1989), and delimits a recognized zone of low genetic diversity in many species distributed across the North Island (e.g. Buckley et al., 2010). Potential causes include long-term inundation of the lower North Island (Bunce et al., 2009), Plio-Pleistocene tectonic activity (Pulford and Stern, 2004), Pleistocene restriction of temperate species to northern glacial refugia and recurrent volcanic activity in the central North Island (Alloway et al., 2007). In the South Island, where divergence dates are more recent, the observed geographic partition could be related to uplift of the Southern Alps along the Alpine Fault (King, 2000) or/followed by isolation in glacial refugia on either side of the South Island (Fig. 6b; Marske et al., 2009). Divergence dates for both species suggest that the tectonic evolution of New Zealand had a greater impact on genetic diversity than more recent climatic crises, although isolation in multiple glacial refugia would have maintained tectonically-driven phylogeographic patterns and exacerbated the accruement of unique substitutions among distant populations. Recent colonization of the Chatham Islands by lineages from the South Island is consistent with results from other studies (e.g., Shepherd et al., 2009).

The remarkable level of genetic diversity identified in *E. lawsoni*, *P. bakewelli* and the mite-harvestman *A. denticulata*, compared to winged beetle species from forest litter microhabitats [*Brachynopus scutellaris* (Redtenbacher), Leschen et al., 2008; *A. labralis*, Marske et al., 2009] suggests that we know very little about the comparative evolution of the litter invertebrate fauna. The distribution of this diversity is also different: for *A. labralis*, genetic diversity among and within clades is concentrated along the South Island's west coast (Marske et al., 2009), which contains New Zealand's greatest extent of continuous native forest, while for the two Zopheridae, genetic diversity is clustered around Cook Strait. Our results highlight that even among species with similar ecological requirements and modern distributions, vicariance, habitat fragmentation and dispersal can result in very different evolutionary histories, particularly in geologically dynamic environments, a phenomenon which is becoming increasingly apparent as more phylogenetic data become available (e.g., Spencer et al., 2006; Pons et al., submitted for publication). Addressing the origins of the biota in these evolutionary theatres will require integrating the methods of multiple disciplines and data from a wide variety of species (Waltari et al., 2007; Hickerson et al., 2010).

5. Conclusions

Divergence dates for *E. lawsoni* and *P. bakewelli* are consistent with the topographic evolution of New Zealand over the last ~10–20 Ma, whereas the LGM does not appear to have left a marked signature in the time-scaled phylogeny. Phylogenetic structure and dispersal matrices indicating sustained gene flow suggest that isolation into the projected LGM refugia may have amplified the genetic signal of earlier vicariance. However, strong temporal incongruence between the coalescent dates and the LGM precludes direct comparison of the phylogenetic and ENM results.

Acknowledgments

We thank Margaret Thayer, Al Newton, Dave Clark, John Nunn, Ainsley Seago, Julia Allwood, John Early, Darren Ward, Ken Puliafico, Leonie Clunie and Grace Hall for help with specimens and locality data, and Dilini Attanayake, Robyn Howitt and Duckchul Park for laboratory assistance. Jake Overton, Gary Barker, Craig Briggs, Robbie Price and Fraser Morgan provided advice on ENMs and ArcGIS. Peter Tsai and Philippe Lemey helped with the coalescent analyses. Beetle photos are by Birgit Rhode. Comments on this manuscript were provided by Alfried Vogler and three anonymous referees. Specimens were collected under the Landcare Research Global Concession issued by the Department of Conservation. This research was funded by the Royal Society of New Zealand Marsden Fund (LCR0502) and the Foundation for Research, Science and Technology through the Defining New Zealand's Land Biota OBI, with additional support from the Field Museum of Natural History, the University of Auckland, and the Danish National Research Foundation (to the Center for Macroecology, Evolution and Climate).

Appendix A. Supplementary material

Supplementary data associated with this article can be found, in the online version, at doi:10.1016/j.ympev.2011.01.005.

References

Alloway, B.V., Lowe, D.J., Barrell, D.J.A., Newnham, R.M., Almond, P.C., Augustinus, P.C., Bertler, N.A., Carter, L., Litchfield, N.J., McGlone, M.S., Shulmeister, J., Vandergoes, M.J., Williams, P.W.NZ-INTIMATE Members, 2007. Towards a climate event stratigraphy for New Zealand over the past 30,000 years (NZ-INTIMATE project). J. Quaternary Sci. 22, 9–35.

Ashcroft, M.B., 2010. Identifying refugia from climate change. J. Biogeogr. 37, 1407–1413.

Beyer, H.L., 2004. Hawth's Analysis Tools for ArcGIS. <http://www.spatialecology.com/htools> (accessed 13.07.09).

Boyer, S.L., Baker, J.M., Giribet, G., 2007. Deep genetic divergences in *Aoraki denticulata* (Arachnida, Opiliones, Cyphophthalmi): a widespread 'mite harvestman' defies DNA taxonomy. Mol. Ecol. 16, 4999–5016.

Brower, A.V.Z., 1994. Rapid morphological radiation and convergence in geographical races of the butterfly, *Heliconius erato*, inferred from patterns of mitochondrial DNA evolution. Proc. Natl. Acad. Sci. USA 91, 6491–6495.

Buckley, T.R., Marske, K.M., Attanayake, D., 2009. Identifying glacial refugia in a geographic parthenogen using palaeoclimate modeling and phylogeography: the New Zealand stick insect *Argosarchus horridus* (White). Mol. Ecol. 18, 4650–4663.

Buckley, T.R., Marske, K.M., Attanayake, D., 2010. Phylogeography and ecological niche modelling of the New Zealand stick insect *Clitarchus hookeri* (White) support survival in multiple coastal refugia. J. Biogeogr. 37, 682–695.

Bunce, M., Worthy, T.H., Phillips, M.J., Holdaway, R.N., Willerslev, E., Haile, J., Shapiro, B., Scofield, R.P., Drummond, A., Kamp, P.J.J., Cooper, A., 2009. The evolutionary history of the extinct ratite moa and New Zealand Neogene paleogeography. Proc. Natl. Acad. Sci. USA 106, 20646–20651 (online supplement).

Carstens, B.C., Richards, C.L., 2007. Integrating coalescent and ecological niche modeling in comparative phylogeography. Evolution 61, 1439–1454.

Charlat, S., Duploey, A., Hornett, E.A., Dyson, E.A., Davies, N., Roderick, G.K., Wedell, N., Hurst, G.D.D., 2009. The joint evolutionary histories of *Wolbachia* and mitochondria in *Hypolimnas bolina*. BMC Evol. Biol. 9, 64.

Davison, A., 2000. An East–West distribution of divergent mitochondrial haplotypes in British populations of the land snail, *Cepaea nemoralis* (Pulmonata). Biol. J. Linn. Soc. 70, 697–706.

Drummond, A.J., Rambaut, A., 2007. BEAST: bayesian evolutionary analysis by sampling trees. BMC Evol. Biol. 7, 214.

Edwards, S.V., Beerli, P., 2000. Perspective: gene divergence, population divergence, and the variance in coalescent time in phylogeographic studies. Evolution 54, 1839–1854.

Excoffier, L., Smouse, P., Quattro, J., 1992. Analysis of molecular variance inferred from metric distances among DNA haplotypes: application to human mitochondrial DNA restriction data. Genetics 131, 479–491.

Excoffier, L., Laval, G., Schneider, S., 2005. ARLEQUIN ver. 3.0: an integrated software package for population genetics data analysis. Evol. Bioinform. Online 1, 47–50.

Galtier, N., Nabholz, B., Glémin, S., Hurst, G.D.D., 2009. Mitochondrial DNA as a marker of molecular diversity: a reappraisal. Mol. Ecol. 18, 4541–4550.

Garrick, R.C., Sands, C.J., Rowell, D.M., Tait, N.N., Greenslade, P., Sunnucks, P., 2004. Phylogeography recapitulates topography: very fine-scale local endemism of a saproxylic 'giant' springtail at Tallaganda in the Great Dividing Range of south–east Australia. Mol. Ecol. 13, 3329–3344.

Hickerson, M.J., Carstens, B.C., Cavender-Bares, J., Crandall, K.A., Graham, C.H., Johnson, J.B., Rissler, L., Victoriano, P.F., Yoder, A.D., 2010. Phylogeography's past, present, and future: 10 years after Avise, 2000. Mol. Phylogenet. Evol. 54, 291–301.

Hill, K.B.R., Simon, C., Marshall, D.C., Chambers, G.K., 2009. Surviving glacial ages within the biotic gap: phylogeography of the New Zealand cicada *Maoricicada campbelli*. J. Biogeogr. 36, 675–692.

Ho, S.Y.W., Shapiro, B., Phillips, M.J., Cooper, A., Drummond, A.J., 2007. Evidence for time dependency of molecular rate estimates. Syst. Biol. 56, 515–522.

Hugall, A., Moritz, C., Moussalli, A., Stanisic, J., 2002. Reconciling paleodistribution models and comparative phylogeography in the wet tropics rainforest land snail *Gnarosophia bellendenkerensis*. Proc. Natl. Acad. Sci. USA 99, 6112–6117.

Hutchinson, M.F., 2000. ANUSPLIN, Version 4.1. User Guide. Centre for Resource and Environmental Studies, Australian National University, Canberra, ACT, Australia.

Jensen, J.L., Bohonak, A.J., Kelley, S.T., 2005. Isolation by distance, web service. BMC Genet. 6, 13.

Jesus, F.F., Wilkins, J.F., Solferini, V.N., Wakeley, J., 2006. Expected coalescent times and segregating sites in a model of glacial cycles. Genet. Mol. Res. 5, 466–474.

Kidd, D.M., Ritchie, M.G., 2006. Phylogeographic information systems: putting the geography into phylogeography. J. Biogeogr. 33, 1851–1865.

King, P.R., 2000. Tectonic reconstructions of New Zealand: 40 Ma to the present. New Zeal. J. Geol. Geophys. 43, 611–638.

Koordinates, 2008a. NZ FSMS6 (North Island). <http://koordinates.com/layer/300-nz-fsms6-north-island/>.

Koordinates, 2008b. NZ FSMS6 (South Island). <http://koordinates.com/layer/301-nz-fsms6-south-island/>.

Lambeck, K., Yokoyama, Y., Purcell, T., 2002. Into and out of the Last Glacial Maximum: sea-level change during Oxygen Isotope Stages 3 and 2. Quaternary Sci. Rev. 21, 343–360.

Leathwick, J.R., Wilson, G., Stephens, R.T.T., 1998. Climate Surfaces for New Zealand. Landcare Research Contract Report LC9798/126. Landcare Research, Hamilton. pp. 1–19.

Leathwick, J., Morgan, F., Wilson, G., Rutledge, D., McLeod, M., Johnston, K., 2003. Land Environments of New Zealand: a Technical Guide. David Bateman, Auckland.

Lemey, P., Rambaut, A., Drummond, A.J., Suchard, M.A., 2009. Bayesian phylogeography finds its roots. PLoS Comput. Biol. 5, e1000520.

Leschen, R.A.B., Buckley, T.R., Harman, H.M., Shulmeister, J., 2008. Determining the origin and age of the Westland Beech (*Nothofagus*) gap, New Zealand, using fungus beetle genetics. Mol. Ecol. 17, 1256–1276.

Liu, C., Berry, P.M., Dawson, T.P., Pearson, R.G., 2005. Selecting thresholds of occurrence in the prediction of species distributions. Ecography 28, 385–393.

Mardulyn, P., Mikhailov, Y.V., Pasteels, J.M., 2009. Testing phylogeographic hypotheses in a Euro-Siberian cold-adapted leaf beetle with coalescent simulations. Evolution 63, 2717–2729.

Marske, K.A., Leschen, R.A.B., Barker, G.M., Buckley, T.R., 2009. Phylogeography and ecological niche modeling implicate coastal refugia and trans-alpine dispersal of a New Zealand fungus beetle. Mol. Ecol. 18, 5126–5142.

Naish, T.R., 2005. Preface: New Zealand's shallow-marine record of Pliocene–Pleistocene global sea-level and climate change. J. Roy. Soc. New Zeal. 35, 1–8.

Papadopoulou, A., Anastasiou, I., Vogler, A.P., 2010. Revisiting the insect mitochondrial molecular clock: the Mid-Aegean Trench calibration. Mol. Biol. Evol. 27, 1659–1672.

Pearce, J., Ferrier, S., 2000. Evaluating the predictive performance of habitat models developed using logistic regression. Ecol. Modell. 133, 225–245.

Phillips, S.J., Anderson, R.P., Schapire, R.E., 2006. Maximum entropy modeling of species geographic distributions. Ecol. Modell. 190, 231–259.

Phillips, S.J., Dudík, M., 2008. Modeling of species distributions with Maxent: new extensions and a comprehensive evaluation. Ecography 31, 161–175.

Phillips, S.J., Dudík, M., Elith, J., Graham, C.H., Lehmann, A., Leathwick, J., Ferrier, S., 2009. Sample selection bias and presence-only distribution models: implications for background and pseudo-absence data. Ecol. Appl. 19, 181–197.

Posada, D., Crandall, K.A., 1998. Modeltest: testing the model of DNA substitution. Bioinformatics 14, 817–818.

Pons, J., Fujisawa, T., Claridge, E.M., Savill, R.A., Barraclough, T.G., Vogler, A.P., 2010. Deep mtDNA subdivision within Linnean species in an endemic radiation of tiger beetles from New Zealand (genus *Neocicindela*). Mol. Phylogenet. Evol. submitted for publication.

Pulford, A., Stern, T., 2004. Pliocene exhumation and landscape evolution of central North Island, New Zealand: The role of the upper mantle. J. Geophys. Res. 109, F01016.

Raes, N., ter Steege, H., 2007. A null-model for significance testing of presence-only species distribution models. Ecography 30, 727–736.

Rambaut, A., Drummond, A.J., 2007. Tracer v1.4. <http://beast.bio.ed.ac.uk/Tracer>.

Rogers, G.M., 1989. The nature of the lower North Island floristic gap. New Zeal. J. Bot. 27, 221–241.

Rosenberg, N.A., Norborg, M., 2002. Genealogical trees, coalescent theory and the analysis of genetic polymorphisms. Nat. Rev. Genet. 3, 380–390.

Rozas, J., Sánchez-DelBarrio, J.C., Messeguer, X., Rozas, R., 2003. DnaSP: DNA polymorphism analyses by the coalescent and other methods. Bioinformatics 19, 2496–2497.

Shepherd, L.D., de Lange, P.J., Perrie, L.R., 2009. Multiple colonizations of a remote oceanic archipelago by one species: how common is long-distance dispersal? J. Biogeogr. 36, 1972–1977.

Simon, C., Frati, F., Crespi, B., Liu, H., Flook, P.K., 1994. Evolution, weighting, and phylogenetic utility of mitochondrial gene sequences and a compilation of conserved PCR primers. Ann. Entomol. Soc. Am. 87, 651–701.

Spencer, H.G., Brook, F.J., Kennedy, M., 2006. Phylogeography of Kauri Snails and their allies from Northland, New Zealand (Mollusca: Gastropoda: Rhytididae: Paryphantinae). Mol. Phylogenet. Evol. 38, 835–842.

Sunnucks, P., Blacket, M.J., Taylor, J.M., Sands, C.J., Ciavaglia, S.A., Garrick, R.C., Tait, N.N., Rowell, D.M., Pavlova, A., 2006. A tale of two flatties: different responses of two terrestrial flatworms to past environmental climatic fluctuations at Tallaganda in montane southeastern Australia. Mol. Ecol. 15, 4513–4531.

Swofford, D.L., 1998. PAUP*. Phylogenetic Analysis using Parsimony (*and other methods), Version 4. Sinauer Associates, Sunderland, MA.

Tamura, K., Dudley, J., Nei, M., Kumar, S., 2007. MEGA4: Molecular Evolutionary Genetics Analysis (MEGA) software version 4.0. Mol. Biol. Evol. 24, 1596–1599.

Thomaz, D., Guiller, A., Clarke, B., 1996. Extreme divergence of mitochondrial DNA within species of pulmonate land snails. Proc. Roy. Soc. Lond. B 263, 363–368.

Torricelli, G., Carapelli, A., Convey, P., Nardi, F., Boore, J.L., Frati, F., 2010. High divergence across the whole mitochondrial genome in the "pan-Antarctic" springtail *Friesea grisea*: Evidence for cryptic species? Gene 449, 30–40.

Vandergoes, M.J., Fitzsimons, S.J., 2003. The Last Glacial-Interglacial Transition (LGIT) in south Westland, New Zealand: paleoecological insight into mid-latitude Southern Hemisphere climate change. Quaternary Sci. Rev. 22, 1461–1476.

Veloz, S.D., 2009. Spatially autocorrelated sampling falsely inflates measures of accuracy for presence-only niche models. J. Biogeogr. 36, 2290–2299.

Walcott, R.I., 1979. Plate motion and sheer strain rates in the vicinity of the Southern Alps. In: Walcott, R.I. (Ed.), The Origin of the Southern Alps. Royal Society of New Zealand Bulletin 18, pp. 5–12.

Walczyńska, A., Dańko, M., Kozłowski, J., 2010. The considerable adult size variability in wood feeders is optimal. Ecol. Entomol. 35, 16–24.

Wallis, G.P., Trewick, S.A., 2009. New Zealand phylogeography: evolution on a small continent. Mol. Ecol. 18, 3548–3580.

Waltari, E., Hijmans, R.J., Peterson, A.T., Nyári, Á., Perkins, S., Guralnick, R.P., 2007. Locating Pleistocene refugia: comparing phylogeography and ecological niche model predictions. PLoS ONE 7, e563.

Wardle, P., 1963. Evolution and distribution of the New Zealand flora, as affected by Quaternary climates. New Zeal. J. Bot. 1, 3–17.

Watanabe, Y., Chiba, S., 2001. High within-population mitochondrial DNA variation due to microvicariance and population mixing in the land snail *Euhadra quaesita* (Pulmonata: Bradybaenidae). Mol. Ecol. 10, 2635–2645.

Zink, R.M., Barrowclough, G.F., 2008. Mitochondrial DNA under siege in avian phylogeography. Mol. Ecol. 17, 2107–2121.